

## Centreline velocity decay measurements in low-velocity axisymmetric jets

By TOR G. MALMSTRÖM<sup>1</sup>, ALLAN T. KIRKPATRICK<sup>2</sup>,  
BRIAN CHRISTENSEN<sup>2</sup> AND KEVIN D. KNAPPMILLER<sup>2</sup>

<sup>1</sup>Division of Building Services Engineering, Royal Institute of Technology (KTH),  
S-10044 Stockholm, Sweden

<sup>2</sup>Mechanical Engineering Department, Colorado State University, Fort Collins, CO 80523, USA

(Received 19 August 1993 and in revised form 15 April 1997)

The streamwise velocity profiles of low-velocity isothermal axisymmetric jets from nozzles of different diameters were measured and compared with previous experimental data. The objective of the measurements was to examine the dependence of the diffusion of the jet on the outlet conditions. As the outlet velocity was decreased, the centreline velocity decay coefficient began to decrease at an outlet velocity of about  $6 \text{ m s}^{-1}$ .

### 1. Introduction

The subject of this paper is the centreline velocity decay of low-velocity ( $0\text{--}12 \text{ m s}^{-1}$ ) isothermal axisymmetric turbulent jets from round nozzles. Such jets are used extensively in ventilation and air conditioning applications. They are also a reference case and model for more complex types of jets. It has been found that the decay coefficients of axisymmetric jets at low velocities are sensitive to the outlet conditions, namely the nozzle velocity and area, see e.g. Nottage (1951) and Hussein, Capp & George (1994). Details of the relationship are still unclear, however. The objectives of this paper are to contribute with tests of centreline velocity decay in jets from three nozzles with different diameters and outlet velocities in the range  $2\text{--}12 \text{ m s}^{-1}$ , and with a re-evaluation of some of the results of Nottage (1951).

### 2. Background

Early experimental investigations of the velocity decay in axisymmetric jets include Corrsin (1943), Cleaves & Boelter (1947), Albertson *et al.* (1948), Becher (1949), Nottage (1951) and Wagnanski & Fiedler (1969). More recent measurements are reported in Rodi (1975), List (1980), Panchapakesan & Lumley (1993), and Hussein *et al.* (1994).

The jet can be divided into four zones: the core zone where centreline velocity is equal to the outlet velocity, a transition zone where the centreline velocity starts to decrease, a third zone where transverse velocity profiles at different distances are similar, and a termination zone where centreline velocities rapidly decrease. The first three zones are illustrated in figure 1.

The centreline velocity decay in the third zone of axisymmetric jets is typically modelled by a simple decay equation with a  $1/x$  decay profile:

$$\frac{U_x}{U_o} = K \frac{D}{x - x_p} \quad (1)$$

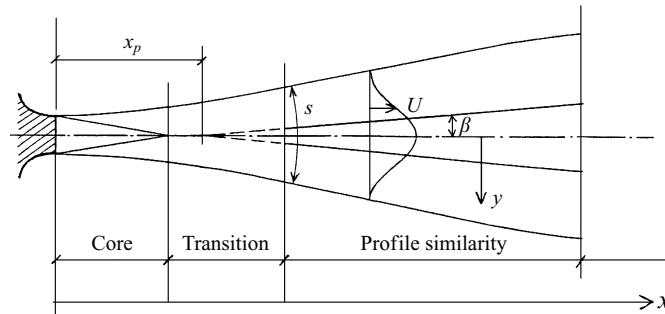


FIGURE 1. Symbols and notation used in the jet model.

In this equation,  $U_x$  is the centreline mean velocity in the  $x$ -direction along the jet axis,  $U_o$  is the outlet velocity of the jet,  $K$  is the velocity decay coefficient,  $D$  is the diameter of the outlet,  $x$  is the coordinate in the axial direction, and  $x_p$  is distance from the nozzle opening to the virtual origin of the jet. The parameter  $x_p$  has a positive value in front of the nozzle.

The transverse velocity profile in the third zone ('profile similarity') of axisymmetric jets is modelled by a Gaussian distribution:

$$\frac{U}{U_x} = e^{-\ln 2 \eta^2}, \quad (2)$$

where  $U$  is the mean velocity in the  $x$ -direction at a point of the jet and  $\eta$  is the non-dimensional transverse coordinate  $y/y_{0.5}$  where  $y$  is the coordinate in the radial direction and  $y_{0.5}$  is the  $y$ -coordinate where  $U/U_x = 0.5$ . The jet is assumed to spread linearly, so  $y_{0.5} = (x - x_p) \tan \beta$ , where  $\beta$  is the half-width spread angle of the jet. For a jet with a Gaussian velocity profile, a 'top hat' velocity profile at the outlet, and a streamwise constant momentum flow rate, the decay coefficient  $K$  is related to the jet spread angle  $\beta$  as follows:

$$K = \frac{(0.5 \ln 2)^{1/2}}{\tan \beta}. \quad (3)$$

Thus equation (2) also can be written

$$\frac{U}{U_x} = e^{-K^2 n^2}, \quad (4)$$

where  $n = y/(x - x_p)$ . Equation (4) relates the  $K$ -value to the transverse velocity profile.

With the above relations, the flow rate at a streamwise distance  $x$  is linearly proportional to  $x$ :

$$\frac{V_x}{V_o} = \frac{2}{K} \frac{x - x_p}{D} = K_v \frac{x - x_p}{D}, \quad (5a)$$

where  $V_x$  is the volume flow rate at distance  $x$ ,  $V_o$  is the volume air flow rate at the outlet, and  $K_v$  is the volumetric flow coefficient.

The Reynolds number ( $Re = U_o D/\nu$ , where  $\nu$  is the kinematic viscosity) is proportional to the square root of the momentum flow rate. Equation (5) thus can be written

$$V_x = \frac{\pi}{4} \frac{2}{K} \nu Re (x - x_p). \quad (5b)$$

	$U_o$ (m s <sup>-1</sup> )	$D$ (cm)	$Re \times 10^{-4}$	$\tan \beta$	$K$	$x_p/D$	$K_v$
Model jet	—	—	—	0.1	5.9	—	0.34
Wynanski & Fiedler (1969)	51	2.54	10	0.086	5.7	3	—
Rodi (1975)	101	1.2	8.7	0.086	5.9	—	—
Panchapakesan & Lumley (1993)	27	0.61	1.1	0.096	6.06	-2.5	—
Hussein <i>et al.</i> (1994) LDA	56.2	2.54	9.55	0.094	5.8	4.0	0.33
Hussein <i>et al.</i> (1994) SHW	56.2	2.54	9.55	0.102	5.9	2.7	0.36

TABLE 1. Comparison of high-velocity axisymmetric jet decay results. The  $K_v$ -values have been integrated by us from the reported transverse velocity profiles.

If  $K$  and  $x_p$  are the same, all jets with identical  $Re$  will have the same volume flow rate at the same distance  $x$  from the outlet.

Frequently cited high-velocity ( $U_o > 12 \text{ m s}^{-1}$ ) measurement results are listed in table 1. Hussein *et al.* (1994) reported both stationary hot wire (SHW) and burst-mode laser-Doppler anemometry (LDA) results. The  $K_v$ -values have been integrated by us from the reported profiles. For comparison, data for the jet model with a Gaussian velocity profile and spread  $\tan \beta = 0.1$  are added. These previous research results indicate that the model gives a good (within 3%) estimate of the actual jet centreline velocity decay, and that the measured  $K$ -values for high-velocity jets are in the range 5.8–6.0.

### 3. Earlier low-velocity jet diffusion measurements

Velocity measurements in high-velocity air jets are difficult owing to the high level of turbulence, as discussed by Hussein *et al.* (1994). The task is even more difficult in low-velocity jets, primarily owing to their instability. Such weak jets tend to move around slightly in the room, sensitive to any disturbance. Even when no disturbance is apparent, the jets are not quite steady. Nottage (1951) describes the process:

... a fixed point in space is swept by a continual succession of billows, vortices, and eddies in addition to the fine-grained fluctuations of turbulence. Boundaries, particularly in the farther regions, may suddenly shift a foot or so and then later return, all without external provocation. No regular frequency has been apparent in any of these behaviors.

Increasing jet spread ( $\tan \beta \sim 1/Re$ ) at low Reynolds number is predicted by Hussein *et al.* Low  $K$ -values (which could indicate increased spread, see equation (3) at low Reynolds numbers ( $Re < 5 \times 10^4$ )) have been reported by Nottage (1951), which seems to be the most extensive study of low-velocity jets so far.

Nottage (1951) obtained jet decay data from a 0.1524 m diameter nozzle with outlet velocities in the range from 0.5 to 30 m s<sup>-1</sup> using a stationary heated thermocouple anemometer. He reported turbulence intensities at the outlet in the range 4–9%, the higher values for lower outlet velocities. This will be discussed later. His tests were made in a space 5.5 m high, 14.4 m wide, and 30 m long. The nozzle centre was located 3.3 m above the floor, 4.4 m from a sidewall, and 7.3 m in front of the endwall. The full width of the space was available for the tests up to a distance of 11 m from the nozzle in the flow direction of the jet, corresponding to 70 nozzle diameters. The length

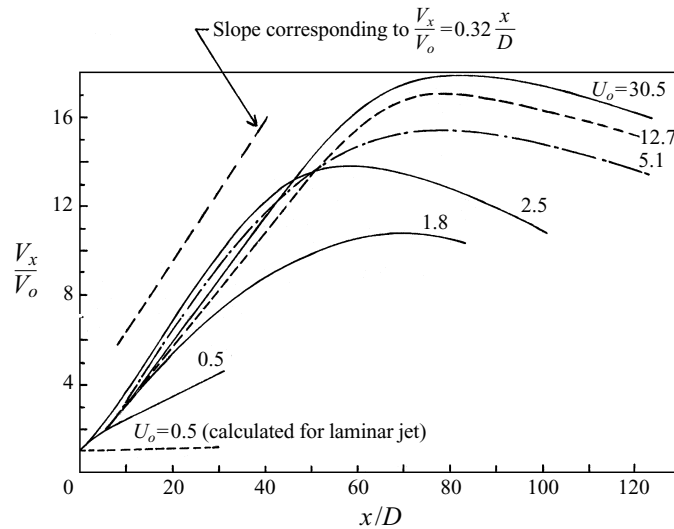


FIGURE 2. Volume flow rates according to Nottage (1951).

corresponding to  $(A_R)^{0.5}$  was 9 m, corresponding to 60 nozzle diameters ( $A_R$  is the room area perpendicular to the jet flow). At distances from the nozzle larger than 11 m, part of the room was blocked. The nozzle was not located in the centre of the room but on the 'centreline' of the unblocked part, which had a value of  $(A_R)^{0.5}$  corresponding to 47 nozzle diameters. The fact that the width of the room was much greater than the height also tended to give the jet an elliptic form for distances from the nozzle larger than 30–40 diameters.

Figure 2 shows flow rates in the jets according to Nottage, calculated from velocity profile measurements. As can be seen from comparison with the reference slope in the figure, corresponding to the results of Ricou & Spalding (1961),  $K_v = 0.32$ , the agreement is good although the results of Nottage are somewhat low. That flow rate ratios decrease at larger distances ( $x/D > 80$  in figure 2, for the high-velocity jets) is natural in this case because of the room blockage mentioned above, but is also consistent with an enclosure effect on confined jets, as discussed by Grititlin (1970), Schneider (1985), Skåret (1987) and Hussein *et al.* (1994). The increase of flow rate is linear, for the high-velocity jets, for  $x/D < 50$  in figure 2. The distances corresponding to  $(A_R)^{0.5}$  and  $1.5(A_R)^{0.5}$  in figures 2 and 3 can be taken as  $x/D = 47$  and 70. These distances have been used by previous authors to characterize the behaviour of confined jets, giving limits for the application of free jet theory, see e.g. ASHRAE Handbook (1993). When velocities are very low, the jet also starts to disintegrate. This causes disturbances at the jet boundary first, and later also in the inner parts of the jet.

Figure 3 shows the centreline velocity decay measured by Nottage. It is striking that the jet with the largest outlet velocity shows a linear slope in the figure up to  $x/D = 120$ , corresponding to  $2.5(A_R)^{0.5}$  and that the jets with low outlet velocities have steeper slopes in the graph, corresponding to lower values of  $K$  in equation (1). Nottage's streamwise and transverse profile data were used by the present authors to obtain  $K$  and  $x_p$  values from least-square fits to the jet decay model represented by equations (1) and (4). For details, see Malmström *et al.* (1992). The results are shown in table 2. Note that the high-velocity ( $30.5 \text{ m s}^{-1}$ ) data of Nottage are in good agreement with the high-velocity results of table 1, especially for the regression interval  $x/D = 20$ –120.

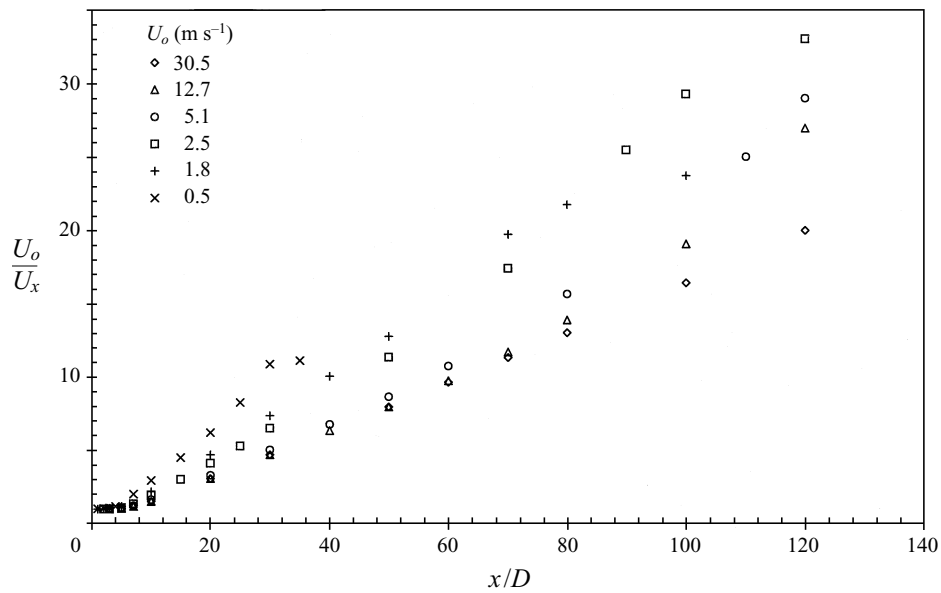


FIGURE 3. Inverse centreline velocities according to Nottage (1951).

$U_o$ (m s <sup>-1</sup> )	$Re$	$K$ equation (4)	Regression interval $x/D$	$K$ Eqn (1)	$x_p/D$ Eqn (1)
30.5	305000	5.9 <sup>a</sup>	20–120	5.92	2.5
		( $x/D = 40$ )	20–70	6.10	1.4
		6.1	20–50	6.17	1.0
12.7	127000	5.6 <sup>a</sup>	20–70	5.87	2.5
		( $x/D = 20$ )	20–50	6.17	1.0
5.1	51000	5.5 <sup>a</sup>	20–60	5.42	2.6
		( $x/D = 30$ )	20–50	5.65	1.5
2.5	25000	4.2	15–50	4.19	2.6
		( $x/D = 20$ )	20–50	3.72	2.6
1.8	18000	4.7 <sup>b</sup>	20–50	3.72	2.6
0.5	5000	— <sup>c</sup>	15–35	2.66	3.2

<sup>a</sup> The two values of  $K$  correspond to the regression intervals in the column to the left, at the same row. Different values of  $x_p$  in the equation (1) regressions, which are used as input for the equation (4) regressions, are the reason for these differences.

<sup>b</sup> According to Nottage, the momentum flow rate  $M_x$  for this jet at  $x/D = 20$  is only 64% of the momentum flow rate  $M_o$  at the outlet. Thus the model is no longer valid and identical values of  $K$  as evaluated with equations (1) and (4) respectively are not possible. Note that a Gaussian velocity profile still is a good approximation.

<sup>c</sup> For this jet, no identical horizontal and vertical profile measurements were available.

TABLE 2. Re-evaluation of measurements of Nottage (1951). Nozzle diameter  $D = 0.1524$  m. The evaluations of  $K$  according to equation (4) have been made for the largest available value of  $x$  where the horizontal and vertical profiles were identical.

As the inverse velocity plots show some upward curvature, the  $K$ -values and  $x_p$ -values determined from the streamwise decay equation (1) are somewhat sensitive to the choice of regression interval. Values corresponding to intervals with  $x/D$  not larger than 50 and not smaller than 15 are used in §5 for comparisons with the new data.

As can be seen from table 2, the mean velocity decay constant  $K$  decreases at lower velocities. This trend is similar for the values of  $K$  calculated from the transverse velocity profiles. Then the outer parts of the profiles, where jet velocities are very low, have been excluded, see figure 4 as an example. This indicates that the lower values of  $K$  are due to increased jet spread, and the jets are disturbed in the outer parts. In the inner part, a Gaussian profile is a good approximation.

The lower  $K$ -values at lower outlet velocities in table 2 could thus be caused by an increased spread of the jet (Malmström 1974). This is, however, not evident in Nottage's measurements of *total* spread angle  $s$  (see figure 1) of the jets, which only increases from  $19.6^\circ$  to  $21.5^\circ$  when  $K$  decreases from 5.9 to 4.2. This is consistent with the result of our re-evaluation mentioned above, that in the inner part of the jet the velocity profile is close to the Gaussian form, and the velocities fall off in the outer part. An explanation is random disturbances at the jet boundary, where jet velocities are very low. Another possible explanation for Nottage's total spread angle results is the unsteadiness of the jet, increasing at low velocities, that has been mentioned earlier. Nottage defined the jet boundary as the location where the flow changed direction (because of room air recirculation), and he measured the location of the boundary directly with smoke filaments. Thus, if the location reported is a mean value, the spread angle  $s$  does not include any influence of movements of the jets. Such movements would decrease the measured mean velocity at a fixed location in the central jet, however.

Figure 2 clearly demonstrates that a change occurs between the two jets with  $U_o = 2.5$  and  $1.8 \text{ m s}^{-1}$  respectively. The lower-velocity jet entrains less air directly upon exiting the nozzle than the higher-velocity jet, breaking the weak trend evident in figure 2 (for  $x/D < 40$ ) toward larger entrainment for lower outlet velocities. According to Nottage the two jets with lowest outlet velocities,  $1.8$  and  $0.5 \text{ m s}^{-1}$ , also started to lose momentum flow rate directly after leaving the nozzle. It was not possible to evaluate  $K$  from the velocity profiles, see table 2. Although it is still possible to evaluate  $K$  from the centreline velocities, the character of the flow apparently is no longer self-preserving turbulent flow.

As mentioned earlier, the turbulence intensity at the outlet was rather high in Nottage's tests and also increased at lower outlet velocities, from about 4.5% at  $12.7 \text{ m s}^{-1}$  to 9% at  $0.5 \text{ m s}^{-1}$ , an increase which could be associated with the change in velocity decay coefficients for the corresponding jets. Nottage made a test with a fine screen in the nozzle entrance, which kept the turbulence intensity at 4.5% even at low outlet velocities. He reports that this caused no change in the tested jet,  $U_o = 1.8 \text{ m s}^{-1}$ , although the outlet turbulence intensity was 4.4% instead of 7.8%. He also applied a 'turbulence promoter' in the nozzle, increasing the turbulence intensity to 9.3%, which had a rather dramatic effect on the  $1.8 \text{ m s}^{-1}$  jet, shifting the location of the virtual origin about seven nozzle diameters upstream, see also Malmström (1974), but apparently not changing the value of  $K$ . The promoter had no effect at  $U_o = 12.7 \text{ m s}^{-1}$ .

In the tests reported by Ricou & Spalding (1961), a jet from a 0.0127 m diameter nozzle expanded in a box with porous walls, and the secondary (i.e. entrainment) flow through the porous wall necessary to avoid a pressure difference between the box and the ambient air was measured. The entrainment flow was measured to a distance of  $x/D = 25.6$ . The volumetric entrainment results are in good agreement with those of

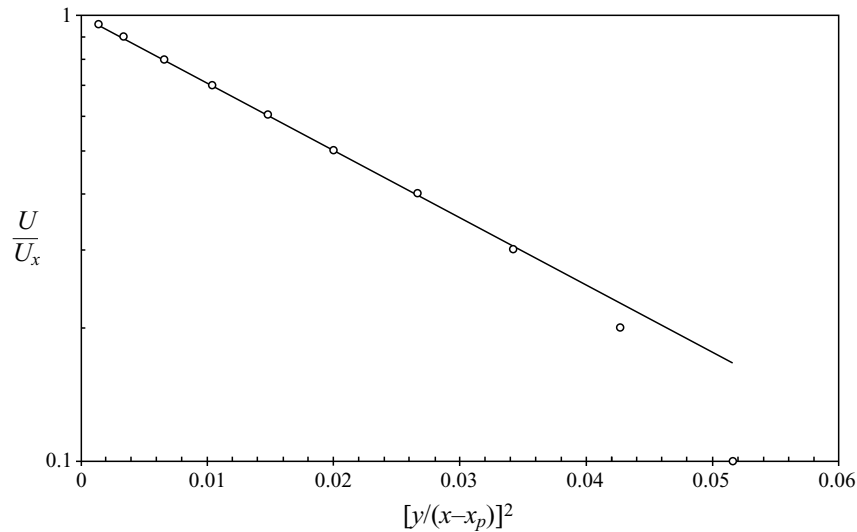


FIGURE 4. Velocity profile at  $x/D = 20$  for Nottage's jet with  $U_o = 2.5 \text{ m s}^{-1}$ . The line shows the corresponding Gauss profile. The two outer measurement points have been excluded from the curve fitting.

Hussein *et al.* (1994) and of Nottage (1951), see table 2 and figure 2. Ricou & Spalding also examined the influence of the outlet Reynolds number on the volumetric entrainment. They found increased entrainment as the Reynolds number is reduced below 25000, a distinct maximum for Reynolds number about 3000 and lower entrainment when the Reynolds number is further decreased.

#### 4. Experimental methodology

An experiment was developed to further examine the influence of the outlet conditions on the jet velocity decay. In order to investigate the problem, experiments were performed with three nozzles, of diameter  $D = 0.1524 \text{ m}$ ,  $0.0758 \text{ m}$ , and  $0.0401 \text{ m}$ , all of the ASME standard long radius type used by Nottage.

The experiments were performed using an experimental set-up consisting of a fan, settling chamber, and nozzle in a large enclosure. A 1 h.p. centrifugal fan with a bypass flow-rate control was used to deliver the required flow rate to the settling chamber. The settling chamber was 1.3 m long, and 0.8 m in diameter. Internal fine mesh screens were used to produce a uniform velocity profile and reduce the turbulence level. The outlet turbulence level was less than 2.5% for the range of measurements. The nozzles with their settling chamber were placed free at one end of a room 12 m long, 7 m wide, and 5 m high. The distance corresponding to  $(A_R)^{0.5}$  was 5.9 m, or 39 diameters for the biggest nozzle ( $D = 0.1524 \text{ m}$ ). The room was instrumented with shielded thermocouple arrays for detection of vertical temperature gradients.

The mean velocity was measured with a Datametrics Model 810 and a TSI Model 1750 constant-temperature anemometer with a single normal wire. The measurement uncertainty of this equipment was  $0.02 \text{ m s}^{-1}$ . An adjustable support was used to move the hot wire along the axis of the jet. The anemometer output was digitized by a Data Translation DT 2801 data acquisition board, and displayed on a 386 PC with ViewDac data acquisition and analysis software. Typical sample times were 180 s, and sample

frequencies were at 10 Hz. The calibration of the anemometer probe was made with two different methods: a small calibration wind tunnel, using a nozzle specially designed for use at low velocities, and with the nozzles used for the jet decay experiments.

The tests were focused on measuring mean centreline velocities for a time interval of 3 minutes. The centreline of the jets had a tendency to slightly move during the tests, and also during individual velocity measurements. This behaviour has been reported earlier (Malmström & Svensson 1971), as have similar observations, like ‘buckling’ and ‘meandering’. It is similar to the observation by Nottage cited above. We used a stationary hot-wire anemometer and had no chance to continuously locate the probe in the moving jet centre (a flying hot wire or a laser-Doppler anemometer would of course do no better). As a consequence of the jet motion, the velocity reading obtained therefore must be lower than the corresponding centreline velocity. Because of this no correction to the reading for turbulence was made, as this would give an even lower velocity.

The check that the chosen probe position really represented the centreline was made by eight slower, hot thermistor probes, arranged in cross-formation and located 0.3 m downstream of the hot-wire probe. The signals were scanned during tests and when it was obvious that the position was wrong, the measurement was repeated after the probe position had been adjusted. It was also repeated if the measured velocity seemed to fall away from the linear trend associated with the zone of self-preserving jet flow in an evaluation graph. Normally every measurement was repeated at least once, even if there appeared to be no need. A measured mean velocity in the jet was never rejected because it was too high. Thus every measured mean velocity reported here is the highest of a varying number recorded at or close to the same location.

It is important to determine the initial momentum carefully, or in this case the corresponding outlet velocity. In our tests, as in those of Nottage, ASME Standard Long Radius Nozzles were used. For standard nozzles, connected to a pressurization chamber with a flow area much bigger than that of the nozzle, as in our tests, the flow coefficient  $\alpha$  approaches 1 at high Reynolds numbers. Then the velocity distribution at the exit of the nozzle is almost a true ‘top hat’ profile and the pressure drop through the nozzle can be used to calculate  $U_o$  and the momentum at the nozzle,  $M_o$ . At lower Reynolds numbers corrections have to be made. In our tests the smallest  $Re$  was about 6500 which indicates flow coefficients in the interval  $0.95 < \alpha < 1$  (ASME flow measurement standard). In the present tests the outlet velocity used for the evaluations was based on the pressure drop through the nozzle. That is the velocity reported in figure 5 and table 3. However, as Nottage used the average outlet velocity when reporting his jet tests, recalculation to average outlet velocity has been made when the present data are compared to his (figure 6 and onward). The largest change is  $0.2 \text{ m s}^{-1}$  occurring at a lowest velocity of  $6.0 \text{ m s}^{-1}$ . The values of the coefficient  $K$  have then been correspondingly adjusted.

## 5. Experimental results

All jet centreline velocity data are contained in figure 5. These overview graphs show a difference in throw for the jets and illustrate the interdependence of  $K$  and  $x_p$ , which is important especially for the low-velocity jets with short throws. The evaluation of the velocity decay coefficient  $K$  and the distance from the centreline velocity equation (1), were made with least-square regressions. The values are listed in table 3. Flow velocities less than  $0.4 \text{ m s}^{-1}$  and test points obviously falling away from the straight line at low

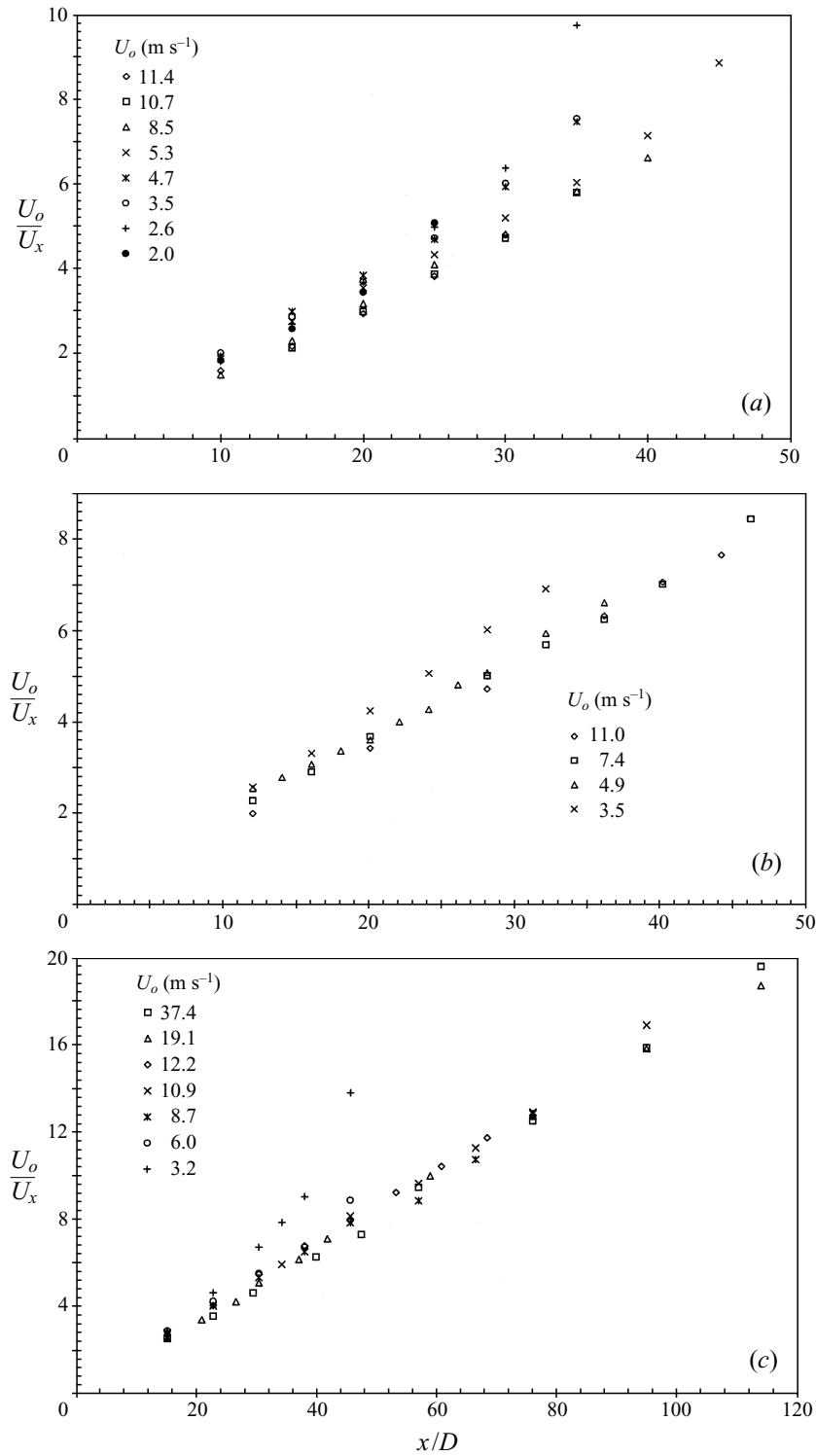


FIGURE 5. Inverted centreline velocity data for all jets tested: (a)  $D = 0.1524$  m (the distance corresponding to  $(A_R)^{0.5}$  is 39 diameters); (b)  $D = 0.0758$  m; (c)  $D = 0.0401$  m.

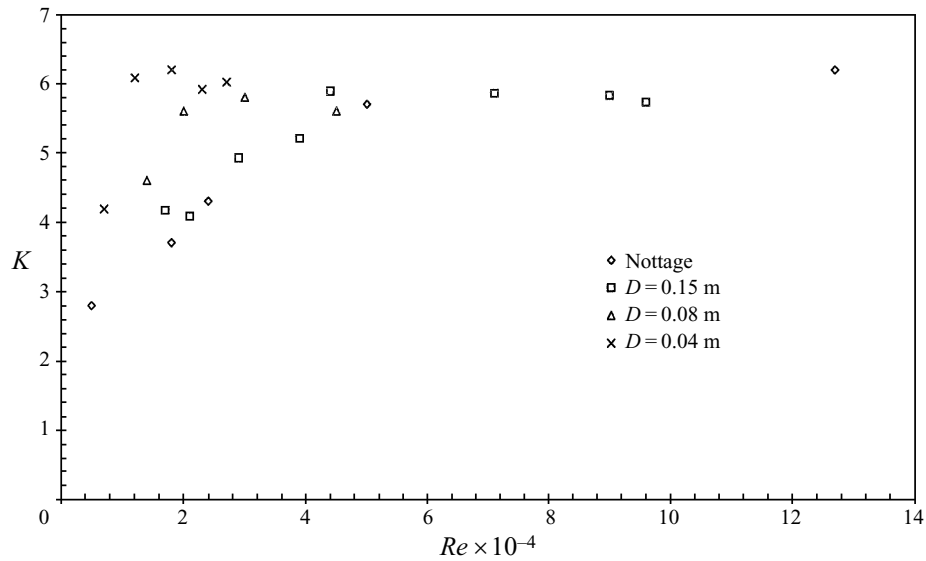


FIGURE 6. Jet centreline velocity decay factor  $K$  versus outlet Reynolds number. Based on average outlet velocities. (Nottage's data are for  $D = 0.15$  m).

Diameter (m)	Reynolds number ( $\times 10^{-4}$ )	$U_o$ ( $\text{m s}^{-1}$ )	Regression interval ( $x/D$ )	$K$ Eqn (1)	$x_p/D$ Eqn (1)
0.1524	9.7	11.4	15–30	5.69	3.0
	9.1	10.7	15–30	5.77	2.7
	7.2	8.5	15–40	5.77	1.7
	4.5	5.3	15–40	5.76	−0.3
	4.0	4.7	15–30	5.14	0.1
	3.0	3.5	15–30	4.76	1.9
	2.2	2.6	15–30	4.04	4.6
	1.7	2.0	15–25	4.01	5.2
	0.0758	4.6	11.0	20–44	5.56
0.0758	3.1	7.4	16–46	5.66	−0.2
	2.1	4.9	16–36	5.54	−0.3
	1.5	3.5	16–32	4.49	1.2
0.0401	8.4	37.4	24–80	5.86	2.8
	4.2	19.1	16–120	6.02	0.0
	2.7	12.2	16–72	5.92	−1.4
	2.4	10.9	16–100	5.77	−0.1
	1.9	8.7	16–80	6.22	−1.6
	1.3	6.0	16–40	5.94	−2.0
	0.7	3.2	16–32	3.98	4.0

TABLE 3. Present measurements of  $K$  and  $x_p$  for nozzles with diameter  $D = 0.15$ , 0.08 and 0.04 m.

velocities have been omitted from the regressions, as the evaluation is for the zone 3 of the jet. Also omitted are test points with  $x > (A_R)^{0.5}$ , where the jets are no longer free, or with  $x/D < 15$ , as the jets are not fully developed there, see Hill (1972).

Figure 6 shows  $K$ -values for the test jet results as a function of outlet Reynolds number. The scatter at low Reynolds numbers is evident. There is no simple dependence on Reynolds number or outlet diameter. Generally, for a given Reynolds

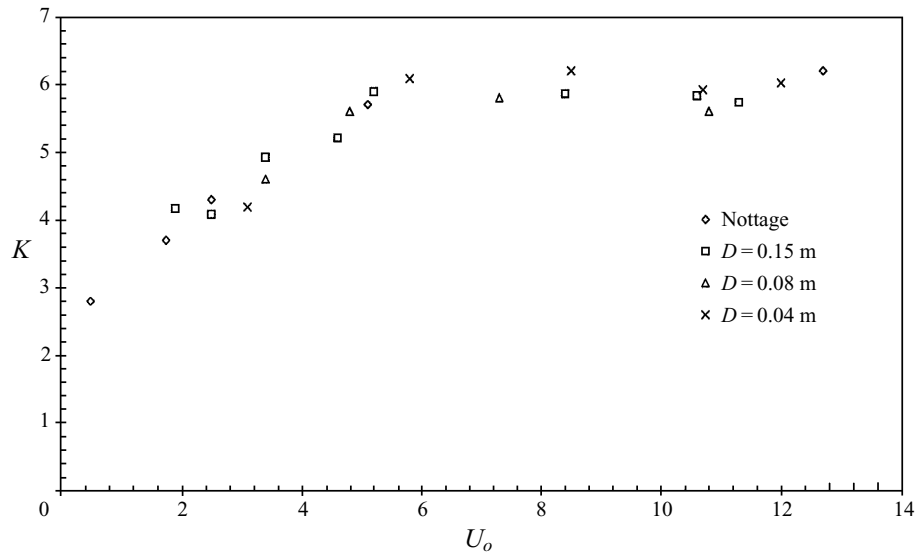


FIGURE 7. Jet centreline velocity decay factor  $K$  versus average outlet velocity.

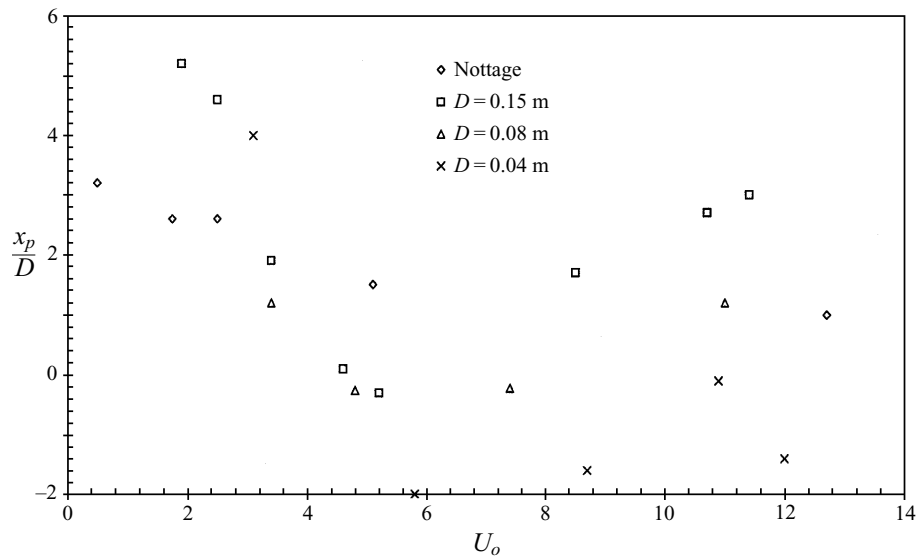


FIGURE 8. Values of  $x_p/D$  as a function of average outlet velocity.

number less than 50000, the decay constant decreases as the outlet diameter is increased, i.e. the outlet velocity is decreased. When the decay constant is plotted versus the outlet velocity  $U_o$  instead of the Reynolds number, the picture looks different, as shown by figure 7. The scatter is much smaller when the outlet velocity is used as the independent variable. The data almost collapse on the same curve. The low-velocity data of Nottage (1951) are also plotted in figures 6 and 7, with good agreement.

It can be argued that our results are caused by jet movements, as discussed in §3. Such movements must have influenced the readings, although the experimental

methodology was designed to minimize this influence. However, for two jets with the same Reynolds number, the expected throw down to a centreline velocity of  $0.4 \text{ m s}^{-1}$  (which is the lowest centreline velocity accepted for regression in the present study) is about the same as the jets have the same momentum flow rate. Also, the expected air flow rates in the jets are the same. Thus there is no reason to expect that the jets would be influenced in different ways by room disturbances causing jet movements. But, of two jets tested with the same low Reynolds number, the one from the larger outlet, which has least initial kinetic energy, has the smaller value of  $K$ , see figure 6 for  $Re < 5 \times 10^4$ .

The value of  $x_p/D$  is about 3–4 for higher velocities, decreases to 0 or  $-1$  for velocities about  $6 \text{ m s}^{-1}$  and then increases when the outlet velocity is further decreased, see figure 8.

## 6. Discussion

The results shown in figures 6 and 7 clearly indicate that for the low-velocity air jets from round nozzles in our and Nottage's tests, the values of the centreline velocity decay coefficient  $K$  decrease at low outlet velocities below  $6 \text{ m s}^{-1}$ . No simple dependence on the outlet Reynolds number is evident and the outlet velocity is a better basis for correlation. The reason for this behaviour is not clear. Figure 8 shows that there is also a variation in the position of the virtual origin of the jets, as evaluated from the centreline velocities. This parameter is known to be influenced by the initial conditions of the jet, for instance reflecting enhanced entrainment just downstream of the nozzle, which shifts the position of the virtual origin upstream. Further downstream the entrainment then returns to 'undisturbed' behaviour, see Crow & Champagne (1971). In our tests, the outlet turbulence could have such an influence. But for the variation in the location of the virtual origin, the outlet velocity  $6 \text{ m s}^{-1}$  was also of central importance in our tests, as there seems to be a minimum in  $x_p/D$  at this velocity, see figure 8.

In order to investigate the influence of this covariation of  $K$  and  $x_p$ , comparisons have been made with flow rates reported by Ricou & Spalding (1961) in their preparatory study about the dependence on Reynolds number. This test was made with a nozzle diameter  $D = 0.0127 \text{ m}$  and the flow rate was measured at a distance of  $x/D = 25.6$ . This is so close to the nozzle that variations in  $x_p$  as well in  $K$  will influence the flow rate, see equation (5a). For the comparison, values of  $V_x/V_o$  at  $x/D = 25.6$  were calculated for the present tests, and for Nottage's tests, with equation (5a), using data from table 2 (for the interval  $x/D = 15$ – $50$ ) and table 3. Nottage's tests with  $U_o = 1.8$  and  $0.5 \text{ m s}^{-1}$  were omitted as equation (5a) is not valid for these cases. Figure 9 shows the result.

Even though the spread is considerable, the trend in the variation of the calculated values with  $U_o$  seems to be similar to that of the measured data. Ricou & Spalding used a nozzle with  $D = 0.0127 \text{ m}$ , and the largest diameter in the present tests was  $0.1524 \text{ m}$ , the same size as Nottage used. If the volume flow rate ratios are plotted instead versus Reynolds number, the spread is bigger and the trends are not similar. However, according to equation (5b),  $V_x$  is a function of Reynolds number. Figure 10 is a corresponding graph, but  $V_x$  has been made dimensionless by dividing by  $D$  and  $\nu$ .

It is evident from figure 10 that the dominating trend is proportionality to Reynolds number. Laminar flow gives a constant value independent of Reynolds number,  $V_x/(D\nu) = 0.06 \times 10^4$ , a value which a linear extrapolation of Ricou & Spalding's data in figure 10 will have at a Reynolds number of about 250. Hussein *et al.* (1994) predict

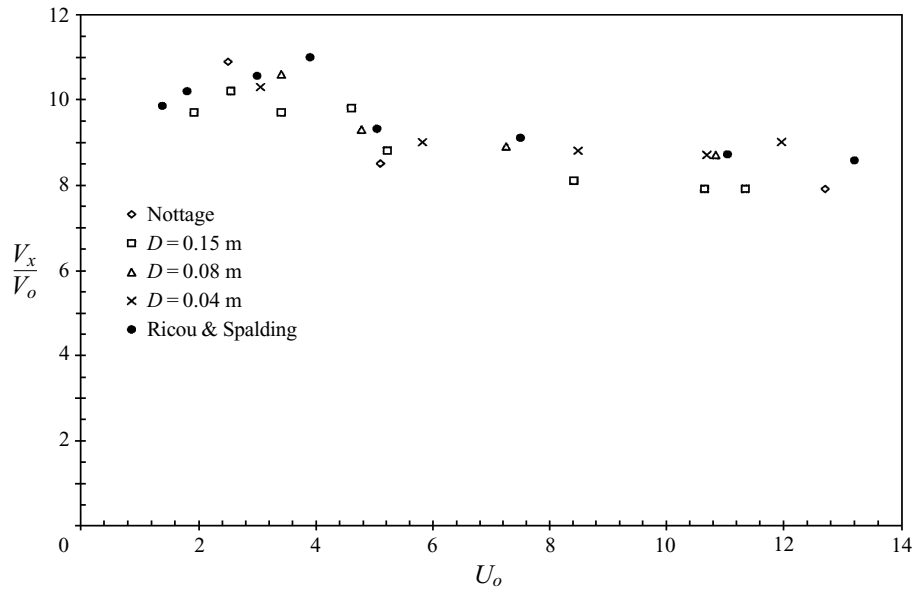


FIGURE 9. Volume flow rates at  $x/D = 25.6$ . Comparison between calculated values and measurements of Ricou & Spalding (1961), who used a nozzle 0.0127 m in diameter.

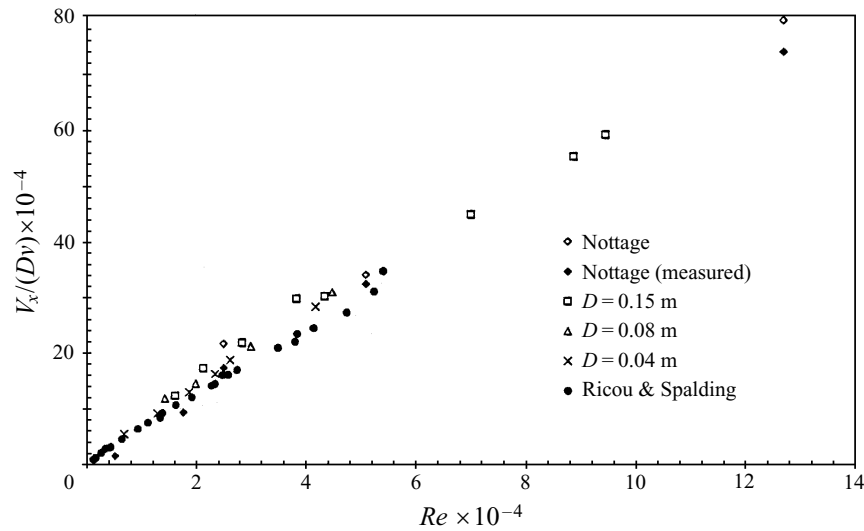


FIGURE 10.  $V_x$  at  $x/D = 25.6$  versus Reynolds number. Open symbols are values calculated with equation (5b), from data such as in figure 9; filled symbols are measured values.

that jets with low Reynolds number, but still fully turbulent, will vary their spread angle  $\beta$  inversely proportionally to Reynolds number, which means that the value of the velocity decay coefficient  $K$  will vary proportionally to Reynolds number, see equation (3). This would also result in a constant value of  $V_x$ , see equation (5b), provided  $x_p$  does not vary. Figure 10, where the lowest Reynolds number is about 1000, shows no sign of such a tendency. However, when the outlet velocity of a jet with a low value of the Reynolds number is further decreased, the virtual origin of the jet

can be expected to move downstream from the nozzle due to tendencies to laminar flow in the first part of the jet, compare figure 8 for velocities  $< 6 \text{ m s}^{-1}$ . This could compensate increased entrainment in the ‘turbulent’ part of the jet.

We have found a few more indications in the literature that the outlet velocity might be an important parameter. Crow & Champagne (1971) found that for the range of Reynolds number they tested, jets seemed to be similar for  $U_o > 12 \text{ m s}^{-1}$ , which is the same experience as we had. Dowling & Dimotakis (1990) found for the centreline concentration decay coefficient in gas jets no simple monotonic trend with outlet Reynolds number. Indications that the  $K$ -value varies with the outlet velocity in a manner similar to the present results can be found in the thesis of Sefker (1989) for smaller outlets and nozzles, 8–20 mm. Regarding the variation of  $x_p$ , experiments on an undisturbed jet from a 0.0762 m nozzle (with a laminar boundary layer) reported by Zaman & Hussain (1980) show a decrease of  $x_p/D$  of about two when the outlet velocity is decreased from  $\sim 12$  to  $\sim 6 \text{ m s}^{-1}$  (their figure 2).

## 7. Summary

Free axial isothermal jets from nozzles were examined to study the effect of nozzle diameter and exit velocity on the centreline mean velocity decay of the jet. Previous analysis and experimental data indicate that the  $K$ -value, which is a characteristic of the centreline velocity decay, decreases at low outlet Reynolds numbers. Re-evaluation of the results of Nottage (1951) indicates that this decrease is connected with a corresponding increase of the half-width spread angle  $\beta$  of the jet, down to a  $K$ -value of about four.

New  $K$ -values for jets from nozzles of different sizes were best correlated by the nozzle outlet velocity. However, there was a co-variation between the  $K$ -values and  $x_p$ -values. Calculated volume flow rates, which parameter took this co-variation into account, correlated with Reynolds number.

This work was done at the REPEAT facility, Solar Energy Application Laboratory (SEAL), Colorado State University, during Tor Malmström’s sabbatical, on leave from the Department of Building Services Engineering, R. Inst. of Technology (KTH), Stockholm, Sweden. Additional funding came from EPRI and the National Swedish Board for Building Research. We are grateful to the organizations mentioned, and to the Director of SEAL, Professor Douglas C. Hittle, for making the project possible.

We are also indebted to Professors William K. George and Peter Nielsen for valuable viewpoints on the subject, and to George Davis and Bill DiCrescentis, who made the test equipment.

## REFERENCES

- ALBERTSON, M. L., DAI, U. B., JENSEN, R. A. & ROUSE, H. 1948 Diffusion of submerged jets. *ASCE Proc.* **74**, 10.
- ASHRAE 1993 *ASHRAE Handbook Fundamentals*, Chap. 31, pp. 1–16. Am. Soc. Heating, Refrigerating, and Air Conditioning Engng, Atlanta.
- BECHER, P. 1949 *Om beregning af indblaesningsåbninger*. Gjellerup, København, Denmark.
- CLEEVES, V. & BOELTER, L. M. K. 1947 Isothermal and nonisothermal air-jet investigations. *Chem. Engng Prog.* **43**, 123–134.
- CORRSIN, S. 1943 Investigation of flow in an axially symmetrical heated jet of air. *NACA Wartime Rep.*, ACR 3L23.

- CROW, S. C. & CHAMPAGNE, F. H. 1971 Orderly structure in jet turbulence. *J. Fluid Mech.* **48**, 547–591.
- DOWLING, D. R. & DIMOTAKIS, P. E. 1990 Similarity of the concentration field of gas-phase turbulent jets. *J. Fluid Mech.* **218**, 109–141.
- GRIMITLIN, M. 1970 Zuluftverteilung in Räumen. *Luft-und Kältetechnik* **5**, 247–257.
- HILL, B. J. 1972 Measurement of local entrainment rate in the initial region of axisymmetric turbulent air jets. *J. Fluid Mech.* **51**, 773–779.
- HUSSEIN, H. J., CAPP, S. P. & GEORGE, W. K. 1994 Velocity measurements in a high Reynolds number, momentum conserving, axisymmetric, turbulent jet. *J. Fluid Mech.* **258**, 31–75.
- LIST, E. J. 1980 Mechanics of turbulent buoyant jets and plumes. In *Turbulent Buoyant Jets and Plumes* (ed. W. Rodi). Pergamon.
- MALMSTRÖM, T.-G. 1974 Om funktionen hos tilluftsgaller. *TM 49*. Department for Heating and Ventilation, KTH, Stockholm, Sweden.
- MALMSTRÖM, T.-G., CHRISTENSEN, B., KIRKPATRICK, A. T. & KNAPPMILLER, K. 1992 Low velocity jets from round nozzles. *Bulletin 26*. Department for Building Services Engineering, KTH, Stockholm, Sweden.
- MALMSTRÖM, T.-G. & SVENSSON, A. 1971 Hastighetsmätningar i ventilationsluftstrålar. *Tidskriften VVS 8*, Stockholm, Sweden.
- NOTTAGE, H. B. 1951 Report on ventilation jets in room air distribution. Case Inst. of Technology, Cleveland, Ohio.
- PANCHAPAKESAN, N. R. & LUMLEY, J. L. 1993 Turbulence measurements in axisymmetric jets of air and helium. Part 1. Air jet. *J. Fluid Mech.* **246**, 197–223.
- RICOU, F. P. & SPALDING, D. B. 1961 Measurements of entrainment by axisymmetrical turbulent jets. *J. Fluid Mech.* **11**, 21–32.
- RODI, W. 1975 A review of experimental data of uniform density free turbulent boundary layers. In *Studies in Convection* (ed. B. E. Launder), pp. 79–165. Academic.
- SCHNEIDER, W. 1985 Decay of momentum flux in submerged jets. *J. Fluid Mech.* **154**, 91–110.
- SEFKER, T. 1989 Verallgemeinerte Darstellung des Verhaltens isothermer Freistrahlen. *Forschungsberichte des Deutschen Kälte- und Klimatechnischen Vereins*, Nr. 27. Stuttgart, Germany.
- SKÅRET, E. 1987 Ventilasjonsteknikk. Kompendium, Institutt for VVS, NTH, Trondheim, Norway.
- WYGNANSKI, I. & FIEDLER, H. E. 1969 Some measurements in the self preserving jet. *J. Fluid Mech.* **38**, 577–612.
- ZAMAN, K. B. M. Q. & HUSSAIN, A. K. M. F. 1980 Vortex pairing in a circular jet. Part 1. *J. Fluid Mech.* **101**, 449–491.